Rotational and Translational Self-Diffusion in Colloidal Sphere Suspensions and the Applicability of Generalized Stokes-Einstein Relations

ARTICLE *in* LANGMUIR · JUNE 2000

Impact Factor: 4.46 · DOI: 10.1021/la000099n · Source: OAI

2 AUTHORS:

Gijsje H Koenderink
FOM Institute AMOLF
91 PUBLICATIONS **2,385** CITATIONS
SEE PROFILE

Albert P Philipse
Utrecht University
189 PUBLICATIONS **6,443** CITATIONS
SEE PROFILE

Rotational and Translational Self-Diffusion in Colloidal Sphere Suspensions and the Applicability of Generalized Stokes−Einstein Relations

Gijsberta H. Koenderink and Albert P. Philipse*

Van't Hoff Laboratory for Physical and Colloid Chemistry, Debye Institute, Utrecht University, Padualaan 8, 3584 CH Utrecht, The Netherlands

Received January 25, 2000. In Final Form: April 3, 2000

We investigate long-time translational and rotational self-diffusion of fluorocarbon tracer spheres (100 nm radius) in aqueous dispersions of silica host spheres (10 nm radius). Diffusion is measured as a function of ionic strength (0−10 mM NaCl) and for host-sphere volume fractions up to 37% using depolarized dynamic light scattering. Both translational and rotational self-diffusion are strongly hindered and have a similar concentration dependence as the low-shear viscosity, except at the lowest ionic strength. Our results show that the Stokes−Einstein (SE) relations, linking viscosity and diffusion at infinite dilution, can be extended to dense colloidal systems whenever the dynamics of the host spheres is fast compared to the experimental time scale. However, when the host-sphere dynamics is relatively slow, such as in the case of very large host particles or charged particles at low ionic strength, tracer-sphere diffusion (in particular rotation) generally is faster than the SE relations.

1. Introduction

A colloidal particle suspended in a liquid executes Brownian motion due to continuous collisions with the solvent molecules. Because of the large size and mass difference between colloidal particles and solvent molecules, the colloid dynamics is several orders of magnitude slower than the solvent dynamics. Therefore, the motion of the colloidal particle can be described in terms of diffusion in a homogeneous solvent with bulk properties such as mass density ρ_0 and shear viscosity η_0.[1−5] On the basis of this approximation the rotational (D_0^r) and translational (D_0^t) diffusion coefficients of a single Brownian particle with radius a are given by the Debye−Stokes−Einstein and the Stokes−Einstein (in short SE) relations respectively[1−5]

$$D_0^{\,r} = \frac{k_B T}{8\pi\eta_0 a^3}, \qquad D_0^{\,t} = \frac{k_B T}{6\pi\eta_0 a} \tag{1}$$

where k_B is Boltzmann's constant and T the absolute temperature. These equations assume stick-boundary conditions at the particle surface.

When a tracer particle diffuses in a concentrated suspension of host particles its motion is affected by potential and hydrodynamic interactions, so the tracer diffusion coefficients are no longer given by eq 1. Furthermore, due to these interactions there is a distinction between a short-time regime ($t < \tau_I$) and a long-time ($t > \tau_I$) regime. In case the tracer and host particles have the same size (i.e., for monodisperse suspensions), the structural relaxation time τ_I is defined as $\tau_I = \xi^2/6D_0^t$; i.e., the time required for one particle to diffuse over a typical interparticle distance ξ. (For hard spheres, ξ approximately equals the particle radius a.) No definition of τ_I has yet been reported for tracers and hosts of different size. Therefore we propose here a definition of τ_I in terms of the relaxation time of the *host* particles, so $\tau_I = \xi_{host}^2/6D_{0,host}^t$; in the short time regime the tracer particle moves in an essentially static cage of host particles, while in the long-time regime it experiences many independent realizations of the host particle configuration. The short-time diffusion coefficients (D_S^t, D_S^r) are therefore purely hydrodynamic quantities,[6] while the long-time diffusion coefficients (D_L^t, D_L^r) are affected also by potential interactions.

Calculations of self-translational[7,8] and rotational[6,9−12] diffusion in concentrated suspensions are complicated by hydrodynamic interactions. Often, these interactions are simply neglected or treated only at the two- or three-body level. An alternative way to model the effect of hydrodynamic interactions on the particle dynamics is to relate the microscopic diffusion coefficients to the macroscopic suspension viscosity. This can be achieved by generalizing the SE relations (eq 1) to concentrated systems, in the short-time regime

$$D_S^{\,r}(\varphi) = \frac{k_B T}{8\pi\eta_\infty'(\varphi)a^3}, \qquad D_S^{\,t}(\varphi) = \frac{k_B T}{6\pi\eta_\infty'(\varphi)a} \tag{2}$$

and in the long-time regime

$$D_L^{\,r}(\varphi) = \frac{k_B T}{8\pi\eta(\varphi)a^3}, \qquad D_L^{\,t}(\varphi) = \frac{k_B T}{6\pi\eta(\varphi)a} \tag{3}$$

The composite system of solvent and host particles is

* To whom all correspondence should be addressed. E-mail: a.p.philipse@chem.uu.nl.

(1) Stokes, G. *Trans. Cambridge Philos. Soc.* **1856**, *9*, 5.
(2) Einstein, A. *Ann. Phys. (Leipzig)* **1906**, *19*, 289.
(3) Einstein, A. *Ann. Phys. (Leipzig)* **1911**, *34*, 591.
(4) Einstein, A. *Investigations on the theory of the Brownian motion*; New York, 1956.
(5) Debye, P. *Polar molecules*; Dover: New York, 1929.
(6) Degiorgio, V.; Piazza, R.; Jones, R. B. *Phys. Rev., E* **1995**, *52*, 2707.
(7) Beenakker, C. W. J.; Mazur, P. *Physica A* **1984**, *126*, 349.
(8) Cichocki, B.; Felderhof, B. U. *J. Chem. Phys.* **1988**, *89*, 3705.
(9) Jones, R. B. *Physica A* **1988**, *150*, 339.
(10) Jones, R. B. *Physica A* **1989**, *157*, 752.
(11) Clercx, H. J. H.; Schram, P. P. J. M. *Physica A* **1991**, *174*, 293.
(12) Clercx, H. J. H.; Schram, P. P. J. M. *J. Chem. Phys.* **1992**, *96*, 3137.

10.1021/la000099n CCC: $19.00
Published on Web 06/02/2000

essentially replaced by an effective structureless fluid with infinite frequency viscosity $\eta_\infty'(\varphi)$ or zero-shear viscosity $\eta(\varphi)$ (with φ the host-particle volume fraction).

Equations 2 and 3, of course, cannot hold quantitatively at low volume fractions, since viscosity and diffusion (at least for hard spheres) have different concentration dependencies. The first-order in φ corrections to η, $D_S{}^r$, $D_S{}^t$, and $D_L{}^r$ are -2.5, -0.63, -1.83, and -2.00 respectively.[13−15] (There are no theoretical results for $D_L{}^r$ yet.) Moreover, the first-order correction to the viscosity is a single-particle property which does not depend on the interaction potential, while the first-order correction on the diffusion coefficients is due to two-particle interactions. At higher volume fractions the situation is less clear, but it has been pointed out that there is no theoretical reason to expect eqs 2 and 3 to hold quantitatively.[13−16] Yet experiments show that for hard spheres translational diffusion has a similar (though not identical) concentration dependence as the relative viscosity. The agreement in the long-time regime[13−15] seems to be better than in the short-time regime,[17−19] as supported by theoretical calculations[20−22] and computer simulations.[20,23,24]

So far, there has been no explicit experimental verification of the SE relations for rotational diffusion. However, comparing measurements[6] of $D_S{}^r/D_0{}^r$ with calculations[22] of η_∞', we conclude that eq 2 is violated for hard spheres; $D_S{}^r\eta_\infty'(\varphi)/D_0{}^r\eta_0$ varies between 1 and 2.7 while $D_S{}^t\eta_\infty'(\varphi)/D_0{}^r\eta_0$ varies only between 1 and 1.3. (Note that for long times, we have no estimate of $D_L{}^r\eta(\varphi)/D_0{}^r\eta_0$.) The effect of electrostatic interactions on the validity of eqs 2 and 3 is likewise not yet clear. Experimental data suggest that for highly charged spheres at low ionic strength the SE relations are violated.[15,19] This is supported by recent mode-coupling theory results[25,26] and Brownian-dynamics simulations.[27]

The central question we want to address here is whether translational and rotational self-diffusion in dense colloidal suspensions have the same (or a similar) concentration dependence as the viscosity, according to eq 3. In view of the assumption underlying eq 3 that the host particle dynamics is (much) faster than the tracer particle dynamics, we expect that increasing the tracer/host size ratio will increase the accuracy of the SE approach. In this paper this hypothesis is checked by experiments on colloidal dispersions of well-defined, charged particles in water, with a tracer/host size ratio of 10. It is shown that $D_L{}^r$ and $D_L{}^t$ are well predicted by the low-shear viscosity of the host suspension, except at low ionic strength where the host-sphere dynamics is slower than the tracer-sphere dynamics.

Self-diffusion of the tracer particles is probed with depolarized dynamic light scattering (DDLS), using optically anisotropic fluorinated polymer particles, used previously by Piazza and co-workers.[27] For host-particles we use silica spheres (Ludox) which are small enough to have a low light scattering intensity in water despite their fairly large refractive index (1.45). Thus, we can perform DDLS experiments at high host-particle volume fractions without multiple scattering. Both tracers and hosts are negatively charged, so the interaction potential can be tuned by varying the ionic strength. The measured self-diffusion coefficients are compared with low-shear viscosities of the Ludox host dispersions, to check the validity of the generalized SE relations.

(De-)polarized Dynamic Light Scattering (DDLS). In this section we briefly recapitulate the theory of depolarized dynamic light scattering (DDLS) from spheres with cylindrically symmetric optical anisotropy. The total electric field scattered by such particles (assuming that the incident electric field is linearly polarized in the vertical direction and the scattering plane is horizontal) is a superposition of two terms. The first is a vertically *polarized* component E_{VV} with amplitude proportional to the optical mismatch between particle and solvent. The second is a *depolarized* component E_{VH} with amplitude proportional to the internal particle anisotropy β, i.e., the difference between the polarizabilities parallel and perpendicular to the optical axis. Polarized and depolarized DLS experiments give the modulus of the correlation functions G_{VV} and G_{VH} respectively:[28]

$$G_{VV}(k,t) = \langle E_{VV}(k,0)E_{VV}^*(k,t)\rangle \tag{4}$$

$$G_{VH}(k,t) = \langle E_{VH}(k,0)E_{VH}^*(k,t)\rangle \tag{5}$$

where the scattering vector $\mathbf{k}$ has a modulus $k = (4\pi n_s/\lambda)\sin(\theta/2)$, θ being the scattering angle, λ the wavelength, and n_s the solvent refractive index. The dynamics of $|G_{VV}|$ reflects mainly the translational diffusion of the particles, while $|G_{VH}|$ is determined both by translational and rotational motion[6]

$$|G_{VV}(k,t)| \propto \sum_{i,j}^{N} \langle e^{ik.[R_i(0)-R_j(t)]}\rangle \tag{6}$$

$$|G_{VH}(k,t)| \propto \beta^2 \sum_{i,j}^{N} \langle [Y_{2,1}[n(0)] + Y_{2,-1}[n(0)]_i[Y_{2,1}[n(t)] + Y_{2,-1}[n(t)]_i\, e^{ik.[R_i(0)-R_j(t)]}\rangle \tag{7}$$

where N is the number of particles within the scattering volume and $R_i(t)$ is the position of the ith particle at time t. The functions $Y_{2,\pm1}$ are spherical harmonics for the orientations of the particle optical axis $\mathbf{n}(t)$. Equations 6 and 7 are often simplified by assuming that orientations of different particles are uncorrelated and that particle translation and rotation are decoupled. The latter approximation is exact for hard spheres at short times.[6,29,30] Furthermore, effects of particle polydis-

(13) Kops-Werkhoven, M. M.; Fijnaut, H. M. *J. Chem. Phys.* **1982**, *77*, 2242.
(14) van Blaaderen, A.; Peetermans, J.; Maret, G.; Dhont, J. K. G. *J. Chem. Phys.* **1992**, *96*, 4591.
(15) Imhof, A.; van Blaaderen, A.; Maret, G.; Dhont, J. G. K. *J. Chem. Phys.* **1994**, *100*, 2170.
(16) Brady, J. F. *Curr. Opin. Colloid Interface Sci.* **1996**, *1*, 472.
(17) Shikata, T.; Pearson, D. S. *J. Rheol.* **1994**, *38*, 601−616.
(18) Zhu, J. X.; Durian, D. J.; Müller, J.; Weitz, D. A.; Pine, D. J. *Phys. Rev. Lett.* **1992**, *68*, 2559.
(19) Bergenholtz, J.; Horn, F. M.; Richtering, W.; Willenbacher, N.; Wagner, N. J. *Phys. Rev. E* **1998**, *58*, R4088.
(20) Ladd, A. J. C. *J. Chem. Phys.* **1990**, *93*, 3484.
(21) Phillips, R. J.; Brady, J. F.; Bossis, G. *Phys. Fluids* **1988**, *31*, 3462.
(22) Beenakker, C. W. J. *Physica A* **1984**, *128*, 48.
(23) Philips, R. J.; Brady, J. F.; Bossis, G. *Phys. Fluids* **1988**, *31*, 3462.
(24) Heyes, D. M.; Mitchell, P. J. *J. Phys. Condens. Matter* **1994**, *6*, 6423.
(25) Banchio, A. J.; Bergenholtz, J.; Nägele, G. *Phys. Rev. Lett.* **1999**, *82*, 1792.
(26) Banchio, A. J.; Nägele, G.; Bergenholtz, J. *J. Chem. Phys.* **1999**. *111*, 8721.
(27) Heyes, D. M.; Branka, A. C. *Phys. Rev. E* **1994**, *50*, 2377.
(28) Dhont, J. K. G. *An introduction to dynamics of colloids*; Elsevier: Amsterdam, 1996.
(29) Hsu, P.; Poulin, P.; Weitz, D. A. *J. Colloid Interface Sci.* **1998**, *200*, 182.
(30) Sohn, D.; Russo, P. S.; Davila, A.; Poche, D. S.; McLaughlin, M. L. *J. Colloid Interface Sci.* **1996**, *177*, 31.

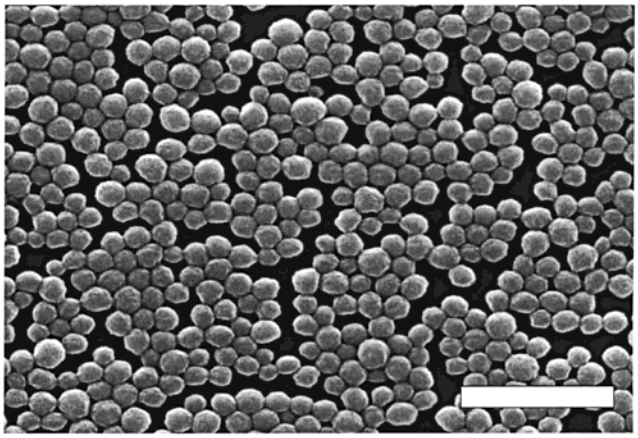

Figure 1. SEM micrograph of PFA tracer particles covered with a 4 nm layer of Pd/Pt. The latex particles are slightly deformed due to the electron beam. The bar denotes 1000 nm.

persity are usually neglected. With these assumptions, $|G_{VV}|$ and $|G_{VH}|$ are reduced to

$$|G_{VV}(t)| \propto N\left[\alpha^2 F_c(k,t) + \frac{4}{15}\beta^2 F_s(k,t)F_r(t)\right] \quad (8)$$

$$|G_{VH}(t)| \propto N\beta^2 F_r(t)F_s(k,t) \quad (9)$$

where $F_r(t)$ and $F_s(k,t)$ are the rotational and translational self-correlation functions

$$F_r(t) = 4\pi\langle Y_{2,1}^*[n(0)]Y_{2,-1}[n(t)]\rangle \quad (10)$$

$$F_s(k,t) = \langle e^{ik.[R_i(0)-R_i(t)]}\rangle \quad (11)$$

and $F_C(k,t)$ is the collective dynamic structure factor which is related to mutual diffusion

$$F_C(k,t) = \langle e^{ik.[R_i(0)-R_j(t)]}\rangle \quad (12)$$

It is clear from eqs 8 and 12 that polarized DLS measures pure self-diffusion only at low particle concentrations, while DDLS always measures purely self-diffusion (eqs 9−11).

At infinite dilution (noninteracting particles) the functions F_s and F_r are exponential for all times, so the first cumulants of $|G_{VV}|$ and $|G_{VV}|$ are given by $\Gamma_{VV} = D_0^t k^2$ and $\Gamma_{VH} = D_0^t k^2 + 6D_0^r$. In the short-time[31,32] ($t < \tau_I$) and long-time[31,32] ($t > \tau_I$) limits the D_0 values are replaced by the short- and long-time diffusion coefficients.

3. Experimental Section

3.1. The Colloidal Model System. The colloidal model system is an aqueous suspension containing fluorocarbon *tracer* particles (PFA) (Figure 1) and silica *host* particles (Ludox AS-40). Ludox host particles were obtained from DuPont as 39 wt % aqueous dispersion stabilized with NaOH (pH 9). The Ludox dispersion was purified by dialysis for 7 days against flowing demineralized water. The final, highly viscous stock dispersion had a volume fraction of 38% and a pH of 9. At this pH, the zeta potential estimated from electrophoresis (Coulter DELSA 440SX) is −35 mV. The silica volume fraction was determined by the weight loss on drying assuming a particle mass density of 2.2 g/cm^3. The average particle radius a_{EM} as determined from transmission electron micrographs (Philips CM10) is 11.0 nm with a standard deviation of 20%.[33]

Table 1. Particle Radius a from Electron Microscopy (EM), DLS, and SLS, Together with Translational (D_0^t) and Rotational (D_0^r) Diffusion Coefficients

particle	a_{EM} (nm)	a_{SLS} (nm)	$D_0^t \times 10^{-12}$ ($m^2 \cdot s^{-1}$)	D_0^r (s^{-1})	a_{DLS} (nm)	a_{DDLS} (nm)
Ludox host	11.0 ± 2.2		27		9.0	
PFA tracer	88 ± 12	102.6	2.63	181.1	93.3	100.5

PFA tracer particles were a kind gift of Ausimont S.p.A. (Milano, Italy). A detailed description of the properties of such particles is given in previous work by Piazza and co-workers.[6,34,35] The latex suspension is prepared in water by dispersion copolymerization of tetrafluoroethylene and perfluoromethylvinyl ether in the presence of an anionic perfluorinated surfactant. The particles have a negative surface charge which is due both to the adsorbed fluorinated surfactant and to the end groups of the polymer chains (fluorinated carboxyl ions) generated by the decomposition of the initiator.

The PFA stock dispersion (34 wt %) was dialyzed for 5 weeks against demineralized water to lower the ionic strength and remove free surfactant. (Dialysis only partially removes the adsorbed fluorinated surfactant.) The zeta potential of the particles after dialysis is −30 mV at pH 5. The particles were inspected with scanning electron microscopy (Philips, XLFEG30 at 10 kV) using a 4 nm Pt/Pd coating to minimize particle damage (shrinkage, collapse, sintering) due to the electron beam. The particles are nearly spherical with an average radius a_{EM} of ca. 88 nm with a standard deviation of 14%. Static light scattering measurements on dilute PFA dispersions were performed on a Fica 50 photometer using vertically polarized light of wavelength 365 nm. The PFA radius a_{SLS} was determined from the position of the first minimum in scattering intensity. The various particle sizes are listed in Table 1. The range in sizes for the different techniques is due to polydispersity.

Hydrodynamic radii (a_{DLS}) of Ludox and PFA particles were determined from the free-particle diffusion coefficients (D_0) measured with dynamic light scattering (DLS) on very dilute dispersions at 25.0 °C with an argon laser source (Spectra Physics model 2000) operating at 514.5 nm (see Table 1).

3.2. Rheological Characterization of the Host Dispersions. Samples for low-shear rheology were prepared by diluting the Ludox stock dispersion with water and adjusting the ionic strength with NaCl. The solution pH varied between 8.5 and 9 depending on the Ludox concentration. The residual ionic strength of the suspensions with no added salt is larger than zero due to the presence of OH^-, particle counterions, and dissolved CO_2. A reasonable estimate is 0.1 mM salt, corresponding to a Debye screening length κ^{-1} of 30 nm. Low-shear viscosity measurements on the Ludox host dispersions were performed using a Contraves Low Shear 40 rheometer equipped with a DIN 412 Couette geometry, thermostated at 25 °C. Viscosities were determined from the slope of shear stress versus shear rate plots. Relative viscosities were obtained by dividing the measured viscosities by the viscosity of the solvent η_0, determined under the same conditions (0.089 mPa·s).

3.3. DDLS Measurements of Tracer Self-Diffusion. Tracer−host sphere mixtures were prepared by addition of a small volume of concentrated tracer stock dispersion to Ludox dispersions with volume fractions between 0 and 38% vol %. The final tracer volume fraction was 0.5% (this does not affect the macroscopic viscosity of the Ludox dispersions), while the final added salt concentration was fixed at 0, 1, or 10 mM NaCl (corresponding to κ^{-1} is ∼30, 10, or 3 nm). Mixtures did not flocculate or gel over periods of at least 7 months. However, if 100 mM NaCl (κ^{-1} is 1 nm) was added, mixtures usually flocculated within 2 days after preparation. This instability may be due to depletion forces induced by the small particles on the larger ones, resulting in a net attraction between the large

(31) Piazza, R.; Degiorgio, V.; Corti, M.; Stavans, J. *Phys. Rev. B* **1990**, *42*, 4885.
(32) Degiorgio, V.; Piazza, R.; Corti, M.; Stavans, J. *J. Chem. Soc., Faraday Trans.* **1991**, *87*, 431.
(33) van Blaaderen, A.; Kentgens, A. P. M. *J. Non-Cryst. Solids* **1992**, *149*, 161.
(34) Piazza, R. *Phys. Scr.* **1992**, *T49*, 94.
(35) Degiorgio, V.; Piazza, R.; Bellini, T. *Adv. Colloid Interface Sci.* **1994**, *48*, 61.

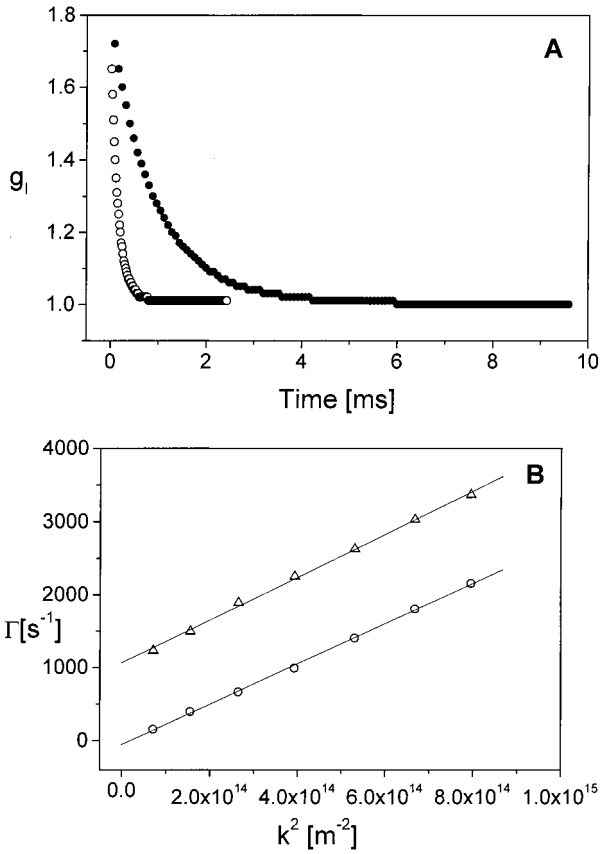

Figure 2. (A) Typical DDLS curves obtained for 0.5% PFA (○) and a mixture of 0.5% PFA and 31.7% Ludox (●) at a scattering angle of 120°. (B) First cumulant as a function of the wavevector squared (k^2) obtained from DLS (○) and DDLS (△) on a 0.5% PFA dispersion. The drawn lines are linear least-squares fits.

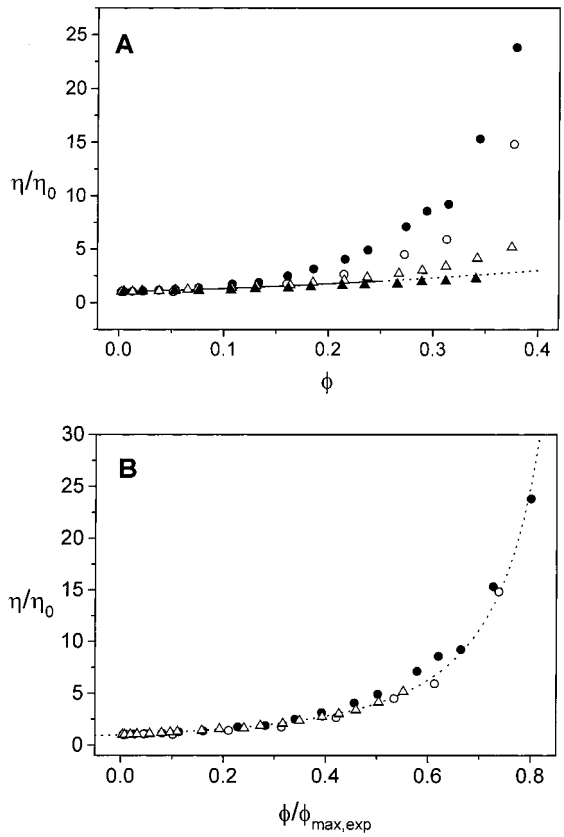

Figure 3. (A) Relative low-shear viscosity of aqueous Ludox host-sphere dispersions with added NaCl concentrations of 0 (●), 1 (○), 10 (△), and 100 (▲) mM. The dotted line shows the theoretical dilute hard-sphere prediction up to order φ^2 (eq 13). (B) Relative viscosity plotted as a function of φ/φ_{max}.

particles. It is important to note that the separate PFA and Ludox dispersions were both stable in the presence of 100 mM NaCl.

DDLS measurements were performed at 25 °C, using a polarized argon laser operating at 500 mW power and a wavelength of 514.5 nm. The incident beam is linearly polarized in the vertical direction. The horizontal (I_{VH}) and vertical (I_{VV}) polarized scattered intensities are measured in the horizontal scattering plane. A sheet polarizer is placed in front of the photomultiplier to select the horizontal component of the scattered intensity. The extinction ratio (better than 10^{-2}) turned out to be sufficient to exclude vertically polarized scattered light. Intensity autocorrelation functions were accumulated with a Malvern 7032 CE, 128 channel correlator, collecting up to 1×10^7 counts for scattering angles (θ) between 30 and 120°. The normalized intensity autocorrelation functions $g_{VH}(k,t)$ were fitted to a standard second-order cumulant expression $g_{VH}(k,t) = \alpha + \beta \exp(-2(\Gamma(k)t + c(k)t^2))$, where α, β, $\Gamma(k)$, and $c(k)$ are used as fitting parameters. In all cases, the full shape of the depolarized correlation functions was a single exponent (see Figure 2A), and the first cumulant $\Gamma(k)$ was a linear function of k^2 (see Figure 2B). $D_L{}^t$ and $D_L{}^r$ were obtained by fitting $\Gamma(k)$ versus k^2 data with a linear least-squares fit (see Figure 2B).

4. Results

4.1. Rheological Characterization of the Host Dispersions. Low-shear viscosities of Ludox host-sphere dispersions with volume fractions up to 38% were obtained from shear stress (σ) versus shear rate ($\dot\gamma$) flow curves measured between 0.01 and 50 s^{-1}. All dispersions with added NaCl (1−100 mM) showed Newtonian behavior, indicating that the microstructure was not significantly disturbed by the shear flow. This is in accordance with the translational Peclet number, $Pe = \dot\gamma a^2/6D_0$, which measures the ratio between the time scale needed to deform the structure by shear ($\dot\gamma^{-1}$) and the time scale of Brownian diffusion that restores it ($\sim a^2/D_0$).[36,37] For the Ludox dispersions, Pe is of order 10^{-5}, i.e., much smaller than 1, so the suspension microstructure is dominated by Brownian motion. However, dispersions with no added NaCl (κ^{-1} ca. 30 nm) were shear thinning for $\varphi > 20\%$, indicating that in these dispersions the time scale of Brownian motion is slower than the time scale of shear deformation. Assuming that relaxation of the microstructure occurs by translational self-diffusion,[38] we estimate that $D_S{}^t$ is of order 10^{-16} m^2/s, i.e., 0.04% of the value at infinite dilution in Table 1.

As shown in Figure 3A, the relative viscosity of the Ludox dispersions increases with increasing Ludox volume fraction (φ) and with decreasing ionic strength. The viscosities may be compared with the following theoretical hard-sphere prediction valid up to 20%:

$$\eta(\varphi,\dot\gamma)/\eta_0 = 1 + C_1\varphi + C_2(\dot\gamma)\varphi^2 \qquad (13)$$

The Einstein coefficient C_1, which accounts for the bulk stress due to an isolated particle, is 2.5 for hard spheres.[2,3] The Huggins coefficient C_2 accounts for particle pair interactions. For hard spheres $C_2 = 6.2$ at zero-shear.[39] Both short-range attractions and long-range repulsions lead to an increase of the value of C_2.[40−43]

(36) van der Werff, J. C.; De Kruif, C. G.; Dhont, J. K. G. *Physica A* **1989**, *160*, 205.
(37) van der Werff, J. C.; De Kruif, C. G.; Blom, C.; Mellema, J. *Phys. Rev. A* **1988**, *37*, 4919.
(38) Brady, J. F. *J. Chem. Phys.* **1993**, *99*, 567.
(39) Batchelor, G. K. *J. Fluid Mech.* **1977**, *83*, 97.
(40) Woutersen, A. T. J. M.; De Kruif, C. G. *J. Chem. Phys.* **1991**, *94*, 5739.
(41) Russel, W. B. *J. Chem. Soc., Faraday Trans. 2* **1984**, *80*, 31.
(42) Cichocki, B.; Felderhof, B. U. *J. Chem. Phys.* **1990**, *93*, 4427.
(43) Russel, W. B. *J. Fluid Mech.* **1978**, *85*, 209.

As shown in Figure 3A, at the highest salt concentrations (10 and 100 mM NaCl) the viscosity is similar to the hard-sphere value. Incidentally, this confirms that the Ludox dispersions are stable at these salt concentrations (see section 3.3). For salt concentrations below 10 mM NaCl ($\kappa a \leq 1$), we find that the viscosity is much larger than that predicted for hard spheres. This points to either attractive or repulsive interactions between the particles at low salt concentration.[40−43] From the salt dependence of the viscosity, we conclude that electric double layer repulsions dominate; when salt is added the spheres show more hard-sphere-like behavior because the range of the double layer repulsions is reduced. In the case of attractive particle interactions, salt addition would enhance the viscosity.

Experimental viscosity data are often compared to the following semiempirical expression derived by Quemada[44] and Krieger:[45]

$$\eta(\varphi,\dot{\gamma}) = \left(1 - \frac{\varphi}{\varphi_{\max}(\dot{\gamma})}\right)^{-2} \qquad (14)$$

stating that the viscosity diverges at a volume fraction $\varphi_{\max}$, which for hard spheres at zero shear is equal or close to the random close packing fraction 0.63.[38,46,47] For charged spheres, the volume fraction dependent viscosity has the same functional form. However, the value of $\varphi_{\max}$ is reduced considerably since the double layers effectively increase the particle dimensions.[38,48] Fitting eq 14 to our viscosity data gives $\varphi_{\max,\exp}$ values of 0.47, 0.51, and 0.68 for 0, 1, and 10 mM NaCl, respectively. (The fitting becomes increasingly unreliable as the ionic strength increases since the maximum experimental volume fraction is only 38%.) On replacing the volume fractions in Figure 3A by a rescaled volume fraction $\varphi/\varphi_{\max,\exp}$ (Figure 3B), the viscosity data can be superimposed on a single master curve which coincides with the hard-sphere prediction. This suggests that the viscosity increase with decreasing ionic strength can be accounted for by the extra excluded volume due to electrostatic repulsive interactions. In other words, the charged spheres behave as hard spheres with effective radii $a_{\text{eff}} = a(\varphi_{\max}/\varphi_{\max,\exp})^{1/3}$ varying between 12 and 11 nm depending on ionic strength.

4.2. Tracer-Sphere Diffusion in Host-Sphere Dispersions. Translational and rotational self-diffusion coefficients (normalized by D_0^r and D_0^t) of PFA tracer spheres in Ludox host dispersions are shown in Figure 4 for added NaCl concentrations of 0, 1, and 10 mM. Dispersions with 100 mM NaCl were unstable, as evidenced by the appearance of flocs within 2 days after preparation (see section 3.3). At all salt concentrations studied, both rotational and translational diffusion are strongly hindered by the presence of the Ludox spheres. In the case of translational diffusion, the concentration dependence of D_L^t/D_0^t is similar at 0 and 1 mM NaCl and becomes weaker at 10 mM NaCl. In the case of rotational diffusion, a slightly different ionic strength dependence is observed. Over a large volume fraction range, rotational diffusion at 1 mM added NaCl is slower than at 0 mM added NaCl. However, with 10 mM added NaCl, diffusion is faster than at 1 mM NaCl. It should be noted that the measured diffusion coefficients represent long-time values. The experimental time scale (10^{-3}−10^{-2} s) is much longer than the structural relaxation time of the Ludox host dispersions: $\tau_I = a_{\text{host}}^2/6D_{0,\text{host}}^t$ (since a_{host} is 10 nm and D_0^t is 2.7×10^{-11} m²·s⁻¹, see Table 1).

In Figure 5, we compare the diffusion coefficients from Figure 4 with the inverse relative viscosity of the host dispersions in the absence of tracers (taken from Figure 3A). In case eq 3 applies, the data for D_L/D_0 and $\eta_0/\eta(\varphi)$ should fall on a single curve. At 0 mM added NaCl, both rotation and translation are somewhat less retarded than predicted by the viscosity. However, at NaCl concentrations of 1 and 10 mM, D_L^t/D_0^t and $\eta_0/\eta(\varphi)$ are comparable to one another, while D_L^r/D_0^r is smaller. Deviations from the viscosity prediction can be more easily visualized by plotting the product of D_L/D_0 times $\eta(\varphi)/\eta_0$ versus the host volume fraction

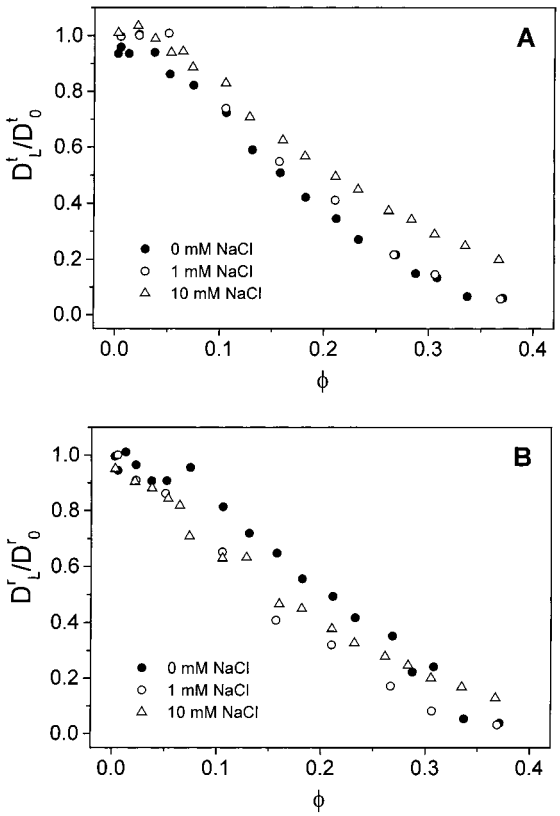

Figure 4. Reduced (A) translational (D_L^t/D_0^t) and (B) rotational (D_L^r/D_0^r) diffusion coefficients as a function of Ludox volume fraction φ, showing the effect of ionic strength.

φ (Figure 6). In case eq 3 applies, this product should equal one over the complete range of volume fractions. In dispersions with 0 mM NaCl both translation ($1 \leq D_L^t\eta(\varphi)/D_0^t\eta_0 \leq 1.4$) and rotation ($1 \leq D_L^r\eta(\varphi)/D_0^r\eta_0 \leq 2.7$) are faster than predicted by eq 3. In dispersions with 1 or 10 mM NaCl, translation more or less coincides with eq 3 ($0.7 \leq D_L^t\eta(\varphi)/D_0^t\eta_0 \leq 1.2$), while rotation is systematically slower than the viscosity prediction ($0.4 \leq D_L^r\eta(\varphi)/D_0^r\eta_0 \leq 1$). Deviations appear to be slightly smaller at the highest salt concentration (10 mM NaCl). In all cases, but especially in the case of 0 mM NaCl, deviations for rotation are larger than those obtained for translation.

5. Discussion

Ionic Strength Dependence of Self-Diffusion. Figures 4 and 5 show that both translational and rotational long-time self-diffusion of large tracer spheres (100 nm radius) is strongly hindered in concentrated aqueous suspensions of small host spheres (10 nm radius). The extent of hindrance is not very sensitive to the ionic strength. Increasing the NaCl concentration (c_s) from 0 to 1 mM does not significantly affect D_L^t/D_0^t. When c_s is further increased to 10 mM, D_L^t/D_0^t increases only slightly. These observations are in accordance with other experimental results for long-time translational diffusion.[14,49] In the case of rotational diffusion, increasing c_s from 0 to 1 mM leads to a small decrease of D_L^r/D_0^r, while increasing c_s further to 10 mM leads to a small enhancement of D_L^r/D_0^r. These observations seem to disagree with previous DDLS measurements of rotational diffusion as a function of ionic strength,[50] which showed that rotational diffusion becomes monotonically slower with increasing ionic

(44) Quemada, D. *Rheol. Acta* **1977**, *16*, 82.
(45) Krieger, I. M. *Adv. Colloid Interface Sci.* **1972**, *3*, 111.
(46) van der Werff, J. C.; De Kruif, C. G .*J. Rheol.* **1989**, *33*, 421.
(47) Jones, D. A. R.; Leary, B.; Boger, D. V. *J. Colloid Interface Sci.* **1992**, *150*, 84.
(48) Russel, W. B.; Saville, D. A.; Schowalter, W. R. *Colloidal dispersions*; Cambridge University Press: Cambridge, 1989.
(49) Bitzer, F.; Palberg, T.; Lowen, H.; Simon, R.; Leiderer, P. *Phys. Rev. E* **1994**, *50*, 2821.
(50) Piazza, R.; Degiorgio, V. *J. Phys.*: *Condens. Matter* **1993**, *5*, B173.

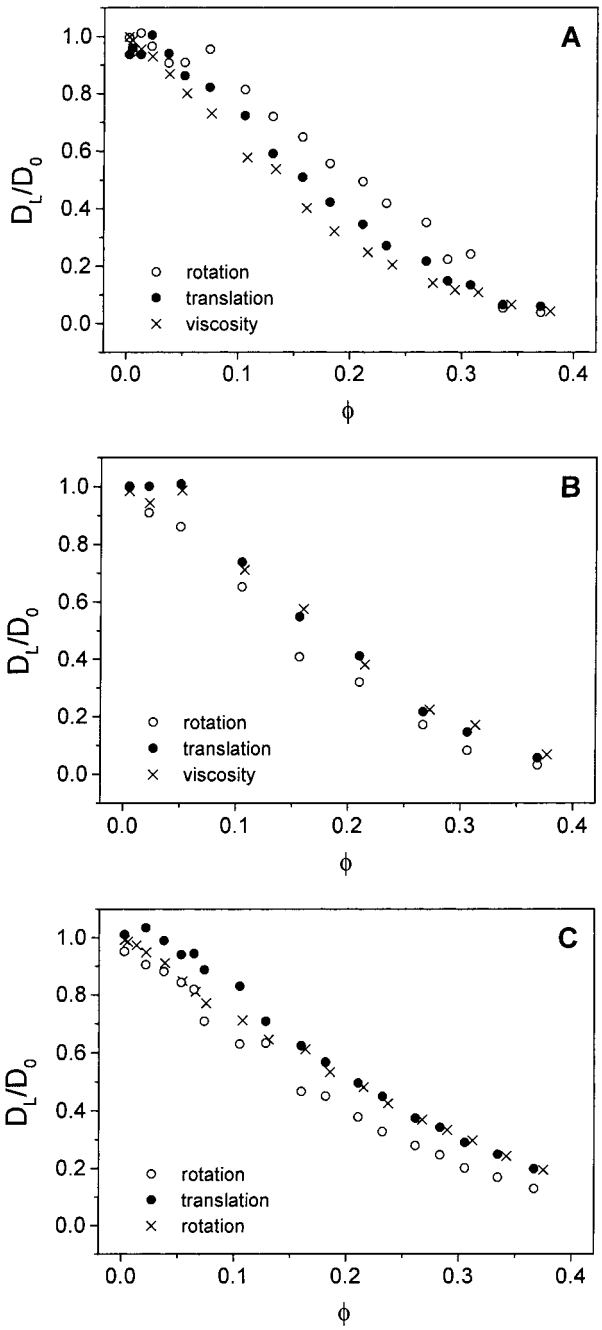

Figure 5. Reduced translational and rotational diffusion coefficients as a function of Ludox volume fraction, for added NaCl concentrations of (A) 0 mM, (B), 1 mM, and (C) 10 mM. Also shown, the inverse relative viscosity (η_0/η) taken from Figure 3.

strength. However, these measurements concerned *short*-time rotation ($\tau_I = 6 \times 10^{-4}$ s), while our measurements concern *long*-time rotation (same experimental time scale, but $\tau_I = 6 \times 10^{-7}$ s).

The previously observed[50] decrease of D_S^r/D_0^r with increasing c_s has been theoretically justified[14,49] by considering the volume fraction dependence of D_S^r/D_0^r. For dilute suspensions one can write $D_S^r/D_0^r = 1 + \lambda^r\varphi + O(\varphi^2)$, where λ^r is a correction given by an average of the hydrodynamic pair interactions (scalar mobility functions) over the equilibrium configuration.[9,51,52] For a monodisperse suspension one obtains

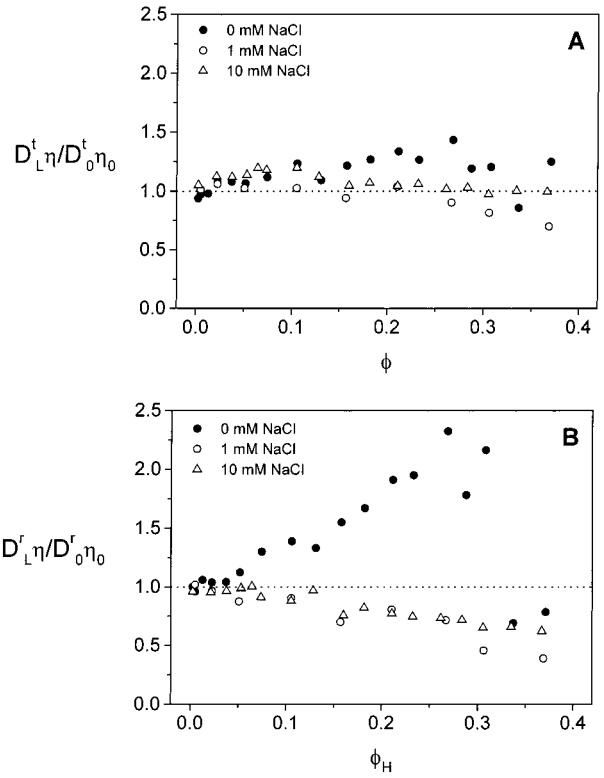

Figure 6. Product of the reduced (A) translational and (B) rotational tracer diffusion coefficients times the relative viscosity of the host-sphere dispersion. The dotted line corresponds to the Stokes−Einstein equation $\eta D_L^t/\eta_0 D_0^t = \eta D_L^r/\eta_0 D_0^r = 1$.

$$\lambda^r = \int_{2a}^{\infty} g(R) 8\pi\eta [\alpha_{11}^{rr}(R) + 2\beta_{11}^{rr}(R)] R^2 \, dR \quad (15)$$

(Note that there is no analogous equation for mixtures of spheres with different sizes in the literature yet.) The mobility functions[14,49] $\alpha_{11}^{rr}(R)$ and $\beta_{11}^{rr}(R)$ are identical for charged and uncharged particles. Since they are rapidly decaying functions of particle separation R, λ^r is very sensitive to the behavior of the radial distribution function $g(R)$ close to the contact distance of two particles. For hard spheres $g(R)$ remains zero up to contact distance $R = 2a$, where it has its principal maximum. As a consequence, lubrication contributions to the hydrodynamic drag play an important role. For charged spheres the electrostatic repulsions shift the principal peak of $g(R)$ to a larger nearest-neighbor separation, reducing lubrication contributions. Thus, when salt is added to a dispersion of charged particles, λ^r (and hence D_S^r/D_0^r) decreases. Incidentally, for D_L^t/D_0^t one can write an expression which is analogous to eq 15, with λ^r is replaced by λ^t.[31,50] However, λ^t is less sensitive to the ionic strength than λ^r because the mobility functions $\alpha_{11}^{tt}(R)$ and $\beta_{11}^{tt}(R)$ decay less rapidly with distance than $\alpha_{11}^{rr}(R)$ and $\beta_{11}^{rr}(R)$.[31,50]

As far as short-time rotational diffusion is concerned, theoretical predictions therefore qualitatively agree with experimental results. With respect to long-time rotational diffusion (D_L^r/D_0^r), no theory has been published yet, in contrast to the many calculations on the translational long-time diffusion coefficient D_L^t. It has been shown[51] that D_L^t/D_0^t can be written in the form

$$D_L^t/D_0^t = 1 + \varphi(\lambda^t + \alpha^t) + O(\varphi^2) \quad (16)$$

with λ^t the short-time correction discussed earlier in this

(51) Cichocki, B.; Felderhof, B. U. *J. Chem. Phys.* **1988**, *89*, 1049.
(52) Watzlawek, M.; Nägele, G. *Physica A* **1997**, *235*, 56.

section and α^t a long-time correction which accounts for the time evolution of the suspension microstructure.[53] Electrostatic repulsions, which enter through the long-time correction α^t, cause D_L^t/D_0^t to be smaller than D_S^t/D_0^t. With increasing ionic strength, both the strength and range of electrostatic repulsions decrease. As a result, α^t increases with ionic strength. Of course at the same time λ^t decreases with increasing ionic strength. Experiments[14,49] have shown that D_L^t/D_0^t monotonically decreases with ionic strength, indicating that the ionic strength dependence of the long-time correction α^t is stronger than that of the short-time correction λ^t.

We conjecture that a similar relation as eq 16 exists also for D_L^r/D_0^r, but with λ^t and α^t replaced by λ^r and α^r:

$$D_L^r/D_0^r = 1 + \varphi(\lambda^r + \alpha^r) + O(\varphi^2) \qquad (17)$$

The parameter λ^r decreases with increasing ionic strength (see eq 15). The ionic strength dependence of α^r is yet unknown. Our experiments suggest that α^r increases with ionic strength: at a low ionic strength salt addition leads to a decrease of D_L^r/D_0^r (probably due to a decrease of λ^r). However, at a higher ionic strength salt addition leads to an increase of D_L^r/D_0^r, which is consistent with an increase of α^r (λ^r monotonically decreases with ionic strength). So our experiments suggest that the salt dependence of long-time rotational diffusion is determined by two opposing effects, namely, short-time contributions (λ^r) and long-time contributions (α^r). It is, of course, clear that calculations or simulations are required to substantiate this explanation, as well as eq 17.

Comparison between Self-Diffusion and Viscosity. The central question in this paper is whether (long-time) translational and rotational self-diffusion in concentrated colloidal suspensions can be (qualitatively) predicted by the SE relations (eq 3), i.e., by the suspension viscosity. At the lowest ionic strength, tracer diffusion (translational and rotational) is faster than predicted by the SE relations ($D_L\eta(\varphi)/D_0\eta_0 \leq 2.7$), as seen from Figures 5 and 6. Thus, the host suspension cannot be treated as an effective fluid. On addition of salt, however, translational and rotational diffusion are in reasonable agreement with the SE prediction, though D_L^r/D_0^r is somewhat smaller than $\eta_0/\eta(\varphi)$. It therefore appears that in the presence of NaCl the effective-fluid picture is, at least qualitatively, applicable.

When salt is added to an initially "salt-free" Ludox host dispersion, the dynamics of the host dispersion changes strongly, as indicated by the rheological experiments (Figure 3). In dispersions with no added salt (in particular for $\varphi > 20\%$), the dynamics of the host particles is strongly restricted. At $\varphi < 20\%$ the host dispersions show Newtonian behavior, but at $\varphi > 20\%$ we find shear thinning. This implies that the structural relaxation time of the host particle configuration becomes slower than the time scale of shearing (roughly 1 s). In section 4.1 we estimated that D^t(host) is of order 10^{-16} m^2/s or less. This is much slower than D^t(tracer), which is of order 10^{-13} m^2/s (see Figure 5A). Thus, on the time scale of tracer diffusion, the host particle configuration is essentially static. However, as soon as some NaCl is added, the host particle dynamics becomes faster: there is no shear thinning over the whole experimental φ range, and the viscosity is reduced.

Combining our findings for tracer diffusion on the one hand and host dynamics on the other hand, we conclude that the colloidal host fluid behaves as an effective fluid when the viscosity is not too large and the host-sphere dynamics are on the same time scale as (or faster than) the tracer-sphere dynamics. If the host-particle dynamics becomes slow relative to the tracer dynamics, then tracer self-diffusion is faster than predicted by the SE relations. This is in qualitative agreement with our study of tracer-sphere diffusion in suspensions of rodlike particles.[54] In this study we found that in dilute rod suspensions tracer-sphere diffusion has the same concentration dependence as the suspension viscosity. However, in entangled, highly viscous, rod suspensions, tracer diffusion is faster than predicted by the viscosity.

At this point it is unclear why rotational diffusion in the presence of NaCl is somewhat smaller than the viscosity prediction ($0.4 \leq D_L^r\eta(\varphi)/D_0^r\eta_0 \leq 1$). This effect could point to aggregation of Ludox onto PFA particles or to aggregation of either PFA or Ludox. However, none of these aggregations appears to occur. DDLS autocorrelation functions, which are very sensitive to aggregation,[55] were single exponential, and decay times were hardly dependent on scattering angle. Attractive interactions between Ludox or PFA particles cannot be ruled out completely. However, attractions, if any, did not measurably affect the viscosity (Figure 3) or tracer translational diffusion (Figure 5).

Generalized SE Relations and (Diffusion) Time Scales. At present there is no (quantitative) theory which predicts or explains the results discussed above. In this section we will therefore present a qualitative picture to account for our findings. Experimental diffusion coefficients reflect the average frictional effect of the surrounding solvent plus host particles on the mobility of the tracer sphere. This average depends on the experimental time window. At very short times the tracer diffusion coefficient reflects mainly the hydrodynamic drag due to the solvent. At very long times, however, the tracer has many statistically independent encounters with host particles, so the diffusion coefficient reflects interactions both with the solvent and with the host particles. Therefore, one expects diffusion to become slower on larger time scales, and also the SE approximation should be more accurate for long-time diffusion than for short-time diffusion. Experiments,[13−15] calculations,[20−22] and computer simulations[20,23,24] indicate that this is indeed the case.

To distinguish between short and long times, the experimental time window should be compared to the host-particle diffusion time scale. If the structural relaxation time of the host particles is small compared to the experimental time scale, then the tracer particle averages in its diffusive motion over the whole space, so its diffusion coefficient reflects the macroscopic viscosity. On the other hand, if the structural relaxation time is large, then the SE relations are violated since the tracer particle cannot access the complete phase space. The tracer sees a discontinuous environment, which, in the limit of zero host mobility, can be called a porous medium. In this case, the viscous drag is closer to the viscosity of the solvent than to the macroscopic viscosity, so tracer motion is faster than predicted by the solution viscosity. This situation occurs for instance in the case of very large host particles[56] or in the case of charge-stabilized suspensions at low salt concentrations, where the host-particle dynamics are very slow due to electrostatic repulsions.

The qualitative distinction between "SE or no SE" discussed above is analogous to the common distinction between short- and long-time self-diffusion,[28] based on

(53) Chichocki, B.; Felderhof, B. U. *J. Chem. Phys.* **1988**, *89*, 3705.

(54) Kluijtmans, S. G. J. M.; Koenderink, G. H.; Philipse, A. P. *Phys. Rev. E* **2000**, *61*, 626.

(55) Vailati, A.; Asnaghi, D.; Giglio, M.; Piazza, R. *Phys. Rev. E* **1993**, *48*, R2358.

(56) Kluijtmans, S. G. J. M.; Philipse, A. P. *Langmuir* **1999**, *15*, 1896.

the interaction time scale $\tau_I = \xi^2/6D_0^t$ (note that we generalized this definition to include situations where tracers and hosts are unequal, to $\tau_I = \xi_{host}^2/6D_{0,host}^t$). The typical nearest-neighbor distance ξ can be estimated by the location of the peak of the radial distribution function $g(R)$. For hard spheres this peak lies at a distance ξ equal to the particle diameter $2a$, while for charged particles ξ will have a larger value[52,57] between the hard-sphere value $\xi = 2a$ and the geometrical mean particle separation $\xi \propto \varphi^{-1/3}$. This means that for charged spheres the structural relaxation time increases with decreasing ionic strength; at a fixed experimental time scale t_{exp} the average environment probed by a tracer particle will be less representative for the host-particle suspension as a whole. Thus the effective viscosity experienced by a tracer will be less in a charge-stabilized suspension than in a hard-sphere suspension. In other words, the SE relations are more likely to be violated for charged than for uncharged particles, in accordance with experiments,[15,19] theory,[25,26] and simulations.[27]

The structural relaxation time is affected not only by the interaction potential but also by the particle size. For larger host particles the structural relaxation time becomes larger relative to the experimental time scale, so the SE relations are also more likely to be violated. Comparing the results from this paper for a tracer/host size ratio of 10 with previous results[13−15] for tracer/host size ratios of 1 confirms that the SE approximations become more accurate when the tracer/host size ratio is increased. This is especially true for rotational diffusion, which seems to deviate more strongly from the SE prediction than translational diffusion, both for monodisperse spheres[13−15] and for bidisperse spheres (see Figure 6). At present the reason for this is not clear. It should be pointed out, however, that a rotating particle needs more time than a translating particle to reach the long-time limit. A rotating particle (which remains at a fixed position during rotation on the rotational time scale) experiences many independent realizations of its environment only if the host particles relax on the experimental time scale. In contrast, a translating particle changes its position during translation, so it experiences a substantial change in its environment even when the host particles do not move very fast. On the basis of these qualitative considerations, we expect that rotational motion becomes slower as the tracer/host particle size increases. This is confirmed by recent simulations by Pagonabarraga.[58] We will investigate this size-ratio dependence in more detail in future experimental studies.

6. Conclusions

We conclude that for the investigated tracer-/host-sphere size ratio of 10, translational and rotational tracer self-diffusion have a similar dependence on the host volume fraction up to at least 38%, irrespective of the ionic strength. Diffusion is more strongly retarded than in the case of a monodisperse sphere suspension. In the presence of NaCl, self-diffusion can be predicted from the macroscopic suspension viscosity by a generalized SE relation. However, at a low ionic strength (ca. 0.1 mM salt), rotation, and to a lesser extent translation, is faster than predicted by the suspension viscosity. This is probably due to the slow dynamics of the strongly interacting host particles, relative to the time scale on which the tracer diffusion coefficient is measured. From a comparison with previous studies on self-diffusion in concentrated colloidal dispersions, we conclude that the accuracy of the SE approximation increases with increasing tracer/host size ratio and with increased screening of electrostatic repulsions. Finally, rotational diffusion deviates more strongly from the suspension viscosity than translational diffusion. The latter aspect should be looked at in more detail by experimental and theoretical investigations.

Acknowledgment. We gratefully acknowledge J. K. G. Dhont, A. van Blaaderen, M. P. Lettinga, G. N. Nägele, and R. Piazza for valuable discussions. We thank B. Kuipers for his help with the DDLS measurements and G. N. Nägele, I. Pagonabarraga, and N. J. Wagner for sending us preprints of their work. This work was supported by The Netherlands Organization for Scientific Research (NWO).

LA000099N

(57) Nägele, G. N.; Watzlawek, M.; Klein, R. *Prog. Colloid Polym. Sci.* **1997**, *107*, 331.

(58) Pagonabarraga, I. Unpublished.